Spontaneous emission spectra and simulating multiple spontaneous generation coherence in a five-level atomic medium

Li Jia-Hua,[1,*] Liu Ji-Bing,[1] Chen Ai-Xi,[2] and Qi Chun-Chao[1]

[1]*Department of Physics, Huazhong University of Science and Technology, Wuhan 430074, People's Republic of China*

[2]*Department of Applied Physics, School of Basic Science, East China Jiaotong University, Nanchang 330013, People's Republic of China*

(Received 15 March 2006; published 21 September 2006)

We investigate the features of the spontaneous emission spectra in a coherently driven cold five-level atomic system by means of a radio frequency (rf) or microwave field driving a hyperfine transition within the ground state. It is shown that a few interesting phenomena such as spectral-line narrowing, spectral-line enhancement, spectral-line suppression, and spontaneous emission quenching can be realized by modulating the frequency and intensity of the rf-driving field in our system. In the dressed-state picture of the coupling and rf-driving fields, we find that this coherently driven atomic system has three close-lying levels so that multiple spontaneously generated coherence (SGC) arises. Our considered atomic model can be found in real atoms, such as rubidium or sodium, so a corresponding experiment can be done to observe the expected phenomena related to SGC reported by Fountoulakis *et al.* [Phys. Rev. A **73**, 033811 (2006)], since no rigorous conditions are required.

DOI: 10.1103/PhysRevA.74.033816 PACS number(s): 42.50.Gy, 32.80.Qk, 32.50.+d

I. INTRODUCTION

In the last few decades there has been intensive interest in the study of spontaneous emission originating from the interaction of the atomic system with the environmental mode. The theoretical approach to the control and modification of spontaneous emission is widely discussed [1–15]. The potential applications for such a spontaneous-emission control cover from lasing without inversion [16–19], high-precision spectroscopy and magnetometry [20–22], transparent high-index materials [23,24], quantum information and computing [25–27], etc. As is well known, for atoms in free space, atomic coherence and quantum interference are the basic phenomena for controlling the spontaneous emission [28,29]. However, it should be noted that the existence of this quantum interference, which is usually referred to as spontaneously generated coherence (SGC) or vacuum-induced coherence (VIC), requires that two close-lying levels be nearly degenerate and that the atomic dipole moments be nonorthogonal when the atom is placed in free space. Unfortunately, it is very difficult, if not impossible, to find a real atomic system with SGC to experimentally realize these phenomena because the rigorous conditions of nearly degenerate levels and nonorthogonal dipole matrix elements cannot be simultaneously satisfied. As a result, few experiments have been performed to achieve these interesting phenomena based on SGC. Recently, Li *et al.* investigated quantum interference between two decay channels of a V-type three-level atom in a multilayer dielectric medium and found that in the anisotropic vacuum, quantum interference could appear even if the two dipole moments were orthogonal to each other [30,31]. More recently, Wu and his coworkers studied the spontaneous-emission properties of a coherently driven four-level atom, and showed a few interesting phenomena, such as fluorescence quenching, spectral-line narrowing, spectral-line enhancement, and spectral-line elimination. They also pointed out that these phenomena could be observed in the experiment since the rigorous condition of nearly degenerate levels with nonorthogonal dipole moments was not required [32]. In the following research [33], Li *et al.* studied a different four-level atomic model and arrived at similar conclusions. In Ref. [34], Fountoulakis *et al.* theoretically investigated coherent effects in a multilevel quantum system that interacts with a single laser pulse and exhibits vacuum-induced coherence effects. They showed that the system possessed two dark states and these dark states could lead to complete population trapping and controllable time-dependent populations. To the best of our knowledge, no further theoretical or experimental work has been carried out to study such atomic spontaneous decay properties in a five-level atomic system in the presence of the double-dark resonances that motivate the current work.

In recent years, a variety of four-level atomic systems driven by three fields have also shown that the probe absorption can be characterized by double-dark resonances [35–43]. For the presence of double-dark resonances, there are basically two different kinds of atomic configuration. One kind is a Λ-configuration system where the final state has twofold levels; the other kind is a tripod atomic system. The interaction of double-dark states has given rise to some original and significant effects. For example, Lukin *et al.* have shown that in a Λ-configuration system where the final state has twofold levels, the interaction of double-dark states can result in a splitting of dark states and the appearance of sharp spectral features [35]. Recently, Gong and his coworkers have shown that in the above Λ-configuration four-level system the presence of double-dark states makes it possible to prepare arbitrary coherent superposition states with equal amplitudes but inverse relative phases, even though the condition of multiphoton resonance is not satisfied [37]. More

*Author to whom correspondence should be addressed. Email address: huajia_li@163.com

recently, they have also proposed high efficiency four-wave mixing induced by double-dark resonances in a five-level system [38]. Yelin *et al.* experimentally show and theoretically confirm that double-dark resonances lead to the possibility of extremely sharp resonances, prevailing even in the presence of considerable Doppler broadening [40]. Alternatively, Goren *et al.* have studied the sub-Doppler and subnatural narrowing of the absorption line induced by interacting dark resonances in a tripod system [42]. Paspalakis *et al.* have analyzed coherent propagation and nonlinear generation dynamics in a coherently prepared four-level tripod system [43].

In this paper, we investigate the spontaneous emission spectra of a coherently driven five-level atomic system with no close-lying levels by means of a radio-frequency (rf) or microwave field driving a hyperfine transition within the ground state. Of particular interest is the application of an rf (or microwave) driving field, as the rf (or microwave) source is more readily available and easier to control in comparison with an extra laser field, and this is the situation considered in this paper. The interesting results are obtained as follows. (i) We show that such interesting phenomena such as spectral-line narrowing, spectral-line enhancement, spectral-line suppression, and spontaneous emission quenching can be realized by modulating the frequency and intensity of the rf field in our system, which are well understood by qualitative explanations in the dressed-state picture of the coupling and rf-driving fields. (ii) We find that this coherently driven atomic system has three close-lying levels in such a dressed-state picture, so that multiple SGC arises. The reason for this is that, with the presence of the coupling and rf-driving fields, before atoms spontaneously decay to the final level, they can go through three different pathways when they are pumped into the uppermost level from the initial level. Thus, the observed singular spontaneous emission spectra can be viewed as results of multiple SGC in the dressed-state picture. Our considered atomic model can be found in real atoms, such as rubidium or sodium, therefore, a corresponding experiment can be done to observe the expected phenomena related to SGC reported by Fountoulakis *et al.* [34], since no rigorous conditions are required again.

It should be noted that the experimental arrangements in our scheme, such as two optical fields, arranged in the form of the Λ-type system, and the rf/microwave driving field connecting one of the ground states with the third state, are similar to those for the double-dark resonances [40], but one of the main differences of these two techniques is the detection method adopted. In a double-resonance technique the optical properties of one of the optical fields are modified, but here the population of the excited state is probed using a spontaneous emission to the fourth ground state. On the other hand, it is noted that the two schemes are for totally different purposes.

Compared with the conventional methods of achieving narrow resonances in the three-level atomic system via optical pumping and electromagnetically induced transparency (EIT) [41], the interaction of dark resonances in our studied system is disturbed by introducing an additional rf or microwave driving field. For the former, EIT width due to optical pumping can be varied via changing the intensities of the driving field and the sharp line can be achieved under the exact condition of the coherent population trapping (CPT). For the latter, the width and amplitude of spectral lines due to spontaneous emission in our present scheme can be changed by tuning either the intensities or frequencies of the microwave driving field, and ultra-narrow lines with greatly enhanced amplitude can be obtained without the above-mentioned CPT condition, which may improve the controllability of the spectral line features with respect to the former. Secondly, our experimental scheme may provide a possibility for realizing multiple SGC in the dressed-state picture because the SGC scheme is hardly realized in real situations.

The paper is organized as follows. In Sec. II, the model is presented. The basic dynamics equations of motion, and their solution for the spontaneous emission spectra are derived. In Sec. III, we analyze our results and discuss in detail the influence of the rf-driving field and the initial probability amplitudes on the spontaneous emission spectra. In Sec. IV, we introduce the dressed-state description of the coupling and rf-driving fields, and demonstrate the possibility for the realization of multiple SGC. Finally, we conclude with a brief summary in Sec. V.

II. MODEL AND SOLUTION

Consider a medium of five-level atoms with one upper, excited level $|3\rangle$ and four lower, ground or metastable levels $|g\rangle$, $|1\rangle$, $|2\rangle$, and $|e\rangle$ as depicted in Fig. 1(a). The excited level $|3\rangle$ is simultaneously coupled to the ground levels $|g\rangle$ and $|2\rangle$ by the coherent probe and coupling laser fields with carrier frequencies of ω_p, ω_c, and Rabi frequencies of $2\Omega_p$, $2\Omega_c$, respectively; while the transition from the excited level $|3\rangle$ to the metastable level $|e\rangle$ is assumed to be coupled by the vacuum modes in the free space. The interaction of driven transitions with the vacuum modes is neglected. The new aspect of the present work is the introduction of an extra coherent field with respect to the model proposed by Wu *et al.* [32], which drives a hyperfine transition between two hyperfine levels $|1\rangle$ and $|2\rangle$. This additional level $|1\rangle$ is also in the ground-state hyperfine structure, therefore the extra field is an rf field with a carrier frequency ω_{rf} and a Rabi frequency $2\Omega_{\mathrm{rf}}$ through an allowed magnetic dipole transition. In the rotating-wave and electrodipole approximations, the whole Hamiltonian describing the atom-field interaction for the system under study in the Schrödinger's picture, is given by

$$H = \sum_{j=1}^{3} \hbar\omega_j|j\rangle\langle j| + \hbar\omega_g|g\rangle\langle g| + \hbar\omega_e|e\rangle\langle e| + \hbar\Big(\Omega_p e^{-i\omega_p t}|3\rangle\langle g| + \Omega_c e^{-i\omega_c t}|3\rangle\langle 2| + \Omega_{\mathrm{rf}} e^{-i\omega_{\mathrm{rf}} t}|2\rangle\langle 1| + \sum_k g_k e^{-i\omega_k t} b_k|3\rangle\langle e| + \mathrm{H.c.}\Big), \quad (1)$$

where the symbol H.c. means the Hermitian conjugate. The quantities Ω_p, Ω_c, and Ω_{rf} are one-half Rabi frequencies for the relevant laser and rf-driven transitions, i.e., Ω_p

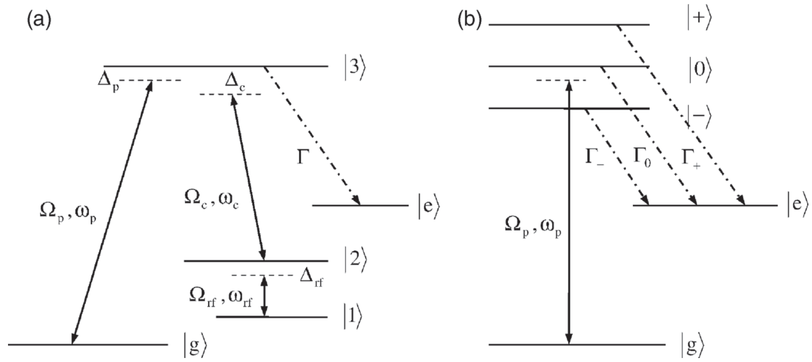

FIG. 1. (a) A schematic diagram of five-level atoms in a coherent medium interacting with a probe laser with Rabi frequency $2\Omega_p$, a coupling laser with Rabi frequency $2\Omega_c$, and a rf-driving field with Rabi frequency $2\Omega_{\rm rf}$ (the transition $|1\rangle \leftrightarrow |2\rangle$ is an electric dipole forbidden transition with magnetic dipole allowed). The atomic levels are labeled as $|g\rangle$, $|1\rangle$, $|2\rangle$, $|3\rangle$, and $|e\rangle$, respectively. This configuration $|1\rangle \rightarrow |2\rangle \rightarrow |3\rangle \rightarrow |g\rangle$ owns the property of double-dark resonances (see Refs. [35,40]). Δ_p, Δ_c, and $\Delta_{\rm rf}$ are the frequency detunings of the corresponding probe, coupling, and rf-driving fields, (see text for details). (b) A corresponding dressed-state description of the coupling and rf-driving laser fields.

$=\mu_{3g}E_p/(2\hbar)$, $\Omega_c=\mu_{32}E_c/(2\hbar)$, and $\Omega_{\rm rf}=\mu_{21}E_{\rm rf}/(2\hbar)$, with $\mu_{mn}=\vec{\mu}_{mn}\cdot\vec{e}_L$ ($\vec{e}_L$ is the unit polarization vector of the corresponding laser field; m, $n=g,1-3$), denoting the dipole moment for the transition between levels $|m\rangle$ and $|n\rangle$, and $E_j^{(a)}=\hbar\omega_j$ ($j=g,1-3$, e) is the energy of the atomic state $|j\rangle$. $b_k^\dagger$ and b_k are, respectively, the creation and annihilation operators for the kth vacuum mode with frequency ω_k; k here represents both the momentum vector and the polarization of the emitted photon. g_k stands for the coupling constant between the kth vacuum mode and the atomic transition $|3\rangle \leftrightarrow |e\rangle$. For the sake of simplicity, in the following analysis we will take $\omega_g=0$ for the ground state $|g\rangle$ as the energy origin. Turning to the interaction picture, the free and interaction Hamiltonian can be rewritten as follows (taking $\hbar=1$) [44,45]

$$H_0 = \omega_p|3\rangle\langle 3| + (\omega_p-\omega_c)|2\rangle\langle 2| + (\omega_p-\omega_c-\omega_{\rm rf})|1\rangle\langle 1| + (\omega_p-\omega_k)|e\rangle\langle e|,$$

$$H_I = \Delta_p|3\rangle\langle 3| + (\Delta_p-\Delta_c)|2\rangle\langle 2| + (\Delta_p-\Delta_c-\Delta_{\rm rf})|1\rangle\langle 1| + (\Delta_p-\delta_k)|e\rangle\langle e| + \left(\Omega_p|3\rangle\langle g| + \Omega_c|3\rangle\langle 2| + \Omega_{\rm rf}|2\rangle\langle 1| + \sum_k g_k b_k|3\rangle\langle e| + \text{H.c.}\right), \quad (2)$$

where we have defined the frequency detunings of the driving fields and the vacuum modes $\Delta_p=\omega_3-\omega_p$, $\Delta_c=\omega_3-\omega_2-\omega_c$, $\Delta_{\rm rf}=\omega_2-\omega_1-\omega_{\rm rf}$, and $\delta_k=\omega_3-\omega_e-\omega_k$, as shown in Fig. 1(a).

The wave function of the atomic system, at a specific time t, can be expanded in terms of the bare-state eigenvectors such that

$$|\Psi(t)\rangle = [a_g(t)|g\rangle + a_1(t)|1\rangle + a_2(t)|2\rangle + a_3(t)|3\rangle]|\{0\}\rangle + \sum_k a_k(t)|e\rangle|1_k\rangle, \quad (3)$$

where $a_j(t)$ ($j=g,1-3$, k) stands for the time-dependent probability amplitude of the atomic state. $|\{0\}\rangle$ represents the absence of photons in all vacuum modes, and $|1_k\rangle$ indicates that there is one photon in the kth vacuum mode.

Making use of the well-known Schrödinger equation in the interaction picture $i\frac{\partial|\Psi(t)\rangle}{\partial t}=H_I|\Psi(t)\rangle$, the coupled equations of motion for the probability amplitude evolution of the atomic wave functions can be readily obtained as

$$\frac{\partial a_g(t)}{\partial t} = -i\Omega_p^* a_3(t), \quad (4a)$$

$$\frac{\partial a_1(t)}{\partial t} = -i(\Delta_p-\Delta_c-\Delta_{\rm rf})a_1(t) - i\Omega_{\rm rf}^* a_2(t), \quad (4b)$$

$$\frac{\partial a_2(t)}{\partial t} = -i(\Delta_p-\Delta_c)a_2(t) - i\Omega_c^* a_3(t) - i\Omega_{\rm rf}a_1(t), \quad (4c)$$

$$\frac{\partial a_3(t)}{\partial t} = -i\left(\Delta_p - i\frac{\Gamma}{2}\right)a_3(t) - i\Omega_p a_g(t) - i\Omega_c a_2(t), \quad (4d)$$

$$\frac{\partial a_k(t)}{\partial t} = -i(\Delta_p-\delta_k)a_k(t) - ig_k^* a_3(t), \quad (4e)$$

where $\Gamma=2\pi|g_k|^2D(\omega_k)$ is the spontaneous-decay rate from level $|3\rangle$ to level $|e\rangle$, and $D(\omega_k)$ is the vacuum-mode density at frequency ω_k in the free space.

Carrying out the Laplace transformations $\tilde{a}_j(s)=\int_0^\infty e^{-st}a_j(t)dt$ [s is the time Laplace transform variable] for Eqs. (4a)–(4e), we have the results

$$s\tilde{a}_g(s) - a_g(0) = -i\Omega_p^*\tilde{a}_3(s), \quad (5a)$$

$$s\tilde{a}_1(s) - a_1(0) = -iw_1\tilde{a}_1(s) - i\Omega_{\rm rf}^*\tilde{a}_2(s), \quad (5b)$$

$$s\tilde{a}_2(s) - a_2(0) = -iw_2\tilde{a}_2(s) - i\Omega_c^*\tilde{a}_3(s) - i\Omega_{\rm rf}\tilde{a}_1(s), \quad (5c)$$

$$s\tilde{a}_3(s) - a_3(0) = -iw_3\tilde{a}_3(s) - i\Omega_p\tilde{a}_g(s) - i\Omega_c\tilde{a}_2(s), \quad (5d)$$

$$s\tilde{a}_k(s) = -iw_4\tilde{a}_k(s) - ig_k^*\tilde{a}_3(s), \quad (5e)$$

where we have introduced the definitions $w_1=\Delta_p-\Delta_c-\Delta_{\rm rf}$, $w_2=\Delta_p-\Delta_c$, $w_3=\Delta_p-i\frac{\Gamma}{2}$, and $w_4=\Delta_p-\delta_k$, respectively. $a_j(0)$ $(j=g,1-3)$ is the probability amplitude at the initial time $t=0$.

Equations (5a)–(5d) can be solved directly in terms of $a_g(0)$, $a_1(0)$, $a_2(0)$, and $a_3(0)$. Therefore, the solution to the probability amplitude $\tilde{a}_3(s)$ can be found as

$$\tilde{a}_3(s)=\frac{f_g(s)a_g(0)+f_1(s)a_1(0)+f_2(s)a_2(0)+f_3(s)a_3(0)}{f(s)}, \tag{6}$$

with

$$f_g(s)=-i[(s+iw_1)(s+iw_2)+|\Omega_{\rm rf}|^2]\Omega_p,$$

$$f_1(s)=-s\Omega_c\Omega_{\rm rf},$$

$$f_2(s)=-is(s+iw_1)\Omega_c,$$

$$f_3(s)=s[(s+iw_1)(s+iw_2)+|\Omega_{\rm rf}|^2],$$

$$f(s)=s(s+iw_3)[(s+iw_1)(s+iw_2)+|\Omega_{\rm rf}|^2]+[(s+iw_1)(s+iw_2)+|\Omega_{\rm rf}|^2]|\Omega_p|^2+s(s+iw_1)|\Omega_c|^2.$$

As is well-known, the spontaneous emission spectra is the Fourier transformation of $\langle E^{-}(t+\tau)E^{+}(t)\rangle_{t\to\infty}$, and can be expressed as the form $S(\delta_k)=\frac{\Gamma}{2\pi|g_k|^2}|a_k(t\to\infty)|^2$ for our studied atomic system. According to the above equation (5e), we have $\tilde{a}_k(s)=\frac{-ig_k^*\tilde{a}_3(s)}{s+iw_4}$. Also, substituting the expression (6) of $\tilde{a}_3(s)$ into the expression of $\tilde{a}_k(s)$, then using the inverse Laplace transformation $a_j(t)=\frac{1}{2\pi i}\int_{\epsilon-i\infty}^{\epsilon+i\infty}e^{st}\tilde{a}_j(s)ds$ [where ϵ is a real number chosen so that $s=\epsilon$ lies to the right of all the singularities (poles and branch cut points) of function $\tilde{a}_j(s)$] and the final-value theorem [46], we can obtain

$$S(\delta_k)=\frac{\Gamma}{2\pi|g_k|^2}|a_k(t\to\infty)|^2=\frac{\Gamma}{2\pi}|\tilde{a}_3(s=-iw_4)|^2=\frac{\Gamma}{2\pi}\left|\frac{f_g(\delta_k)a_g(0)+f_1(\delta_k)a_1(0)+f_2(\delta_k)a_2(0)+f_3(\delta_k)a_3(0)}{f(\delta_k)}\right|^2, \tag{7}$$

where the coefficients are given by

$$f_g(\delta_k)=\Omega_p[(w_4-w_1)(w_4-w_2)-|\Omega_{\rm rf}|^2],$$

$$f_1(\delta_k)=\Omega_c\Omega_{\rm rf}w_4,$$

$$f_2(\delta_k)=\Omega_c w_4(w_4-w_1),$$

$$f_3(\delta_k)=w_4[(w_4-w_1)(w_4-w_2)-|\Omega_{\rm rf}|^2],$$

$$f(\delta_k)=w_4(w_4-w_3)[(w_4-w_1)(w_4-w_2)-|\Omega_{\rm rf}|^2]-|\Omega_p|^2[(w_4-w_1)(w_4-w_2)-|\Omega_{\rm rf}|^2]-|\Omega_c|^2w_4(w_4-w_1),$$

where Eq. (7) is the main result of the present study.

Under the conditions $a_g(0)=1$, $a_1(0)=a_2(0)=a_3(0)=0$, and $\Delta_p=\Delta_c=\Delta_{\rm rf}=0$, we then have $w_1=w_2=0$, $w_3=-i\Gamma/2$, and $w_4=-\delta_k$ in order that the spontaneous emission spectra $S(\delta_k)$ in Eq. (7) can be explicitly expressed in the following form

$$S(\delta_k)=\frac{\Gamma|\Omega_p|^2}{2\pi}\frac{1}{[G-(|\Omega_p|^2+|\Omega_c|^2-|\Omega_{\rm rf}|^2)-|\Omega_c|^2|\Omega_{\rm rf}|^2G^{-1}]^2+\Gamma^2\delta_k^2/4}, \tag{8}$$

where $G=\delta_k^2-|\Omega_{\rm rf}|^2$.

III. RESULTS AND DISCUSSION

In this section, we present a few numerical results about the spontaneous emission spectra $S(\delta_k)$. All parameters used in the following calculations are scaled by γ, which should be in the order of MHz for rubidium or sodium atoms.

First of all, we will analyze how the frequency detuning of the rf-driving field modifies the spontaneous emission spectra $S(\delta_k)$ via the numerical calculations based on Eq. (7). In Fig. 2, we plot the spontaneous emission spectra $S(\delta_k)$ versus the detuning δ_k by modulating frequencies of the rf-driving field under the condition of $a_g(0)=1$ and $a_1(0)=a_2(0)=a_3(0)=0$ when the probe and coupling driving fields are both tuned to the resonant interaction with the atomic transitions $|g\rangle\leftrightarrow|3\rangle$ and $|2\rangle\leftrightarrow|3\rangle$. It is clearly shown that, when the rf-driving field is tuned to level $|2\rangle$ [i.e., $\Delta_{\rm rf}=0$ in Fig. 2(a)], two ultranarrow lines with approximately equal height can be observed on both sides of zero detuning of δ_k. Alternatively, two fluorescence-quenching points are located at $\delta_k=\pm 0.2\gamma$. As a matter of fact, it can be easily seen from Eq. (7) that the generated two fluorescence-quenching points are always located at $\delta_k=\frac{\Delta_{\rm rf}\pm\sqrt{\Delta_{\rm rf}^2+4|\Omega_{\rm rf}|^2}}{2}$, which suggests that the rf field detuning affects the fluorescence-quenching position. From Figs. 2(b)–2(d), we find that the left ultranarrow line can be greatly enhanced, while the right ultranarrow line can be significantly suppressed with the increase of the fre-

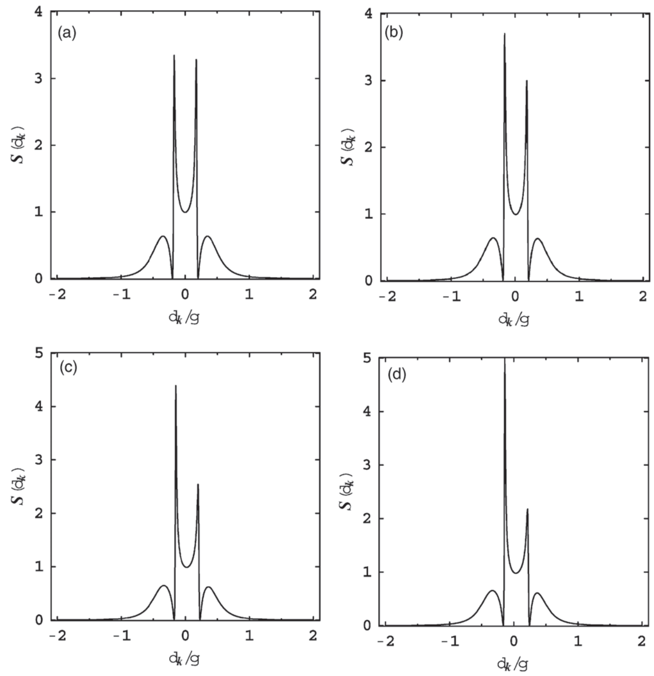

FIG. 2. Spontaneous emission spectra $S(\delta_k)$ (in units of γ^{-1}) for $\Omega_p=0.4\gamma$, $\Omega_c=0.2\gamma$, $\Omega_{\mathrm{rf}}=0.2\gamma$, $a_g(0)=1$, $a_1(0)=a_2(0)=a_3(0)=0$, $\Gamma=\gamma$, $\Delta_p=0$, and $\Delta_c=0$. (a) $\Delta_{\mathrm{rf}}=0$; (b) $\Delta_{\mathrm{rf}}=0.02\gamma$; (c) $\Delta_{\mathrm{rf}}=0.05\gamma$; and (d) $\Delta_{\mathrm{rf}}=0.08\gamma$.

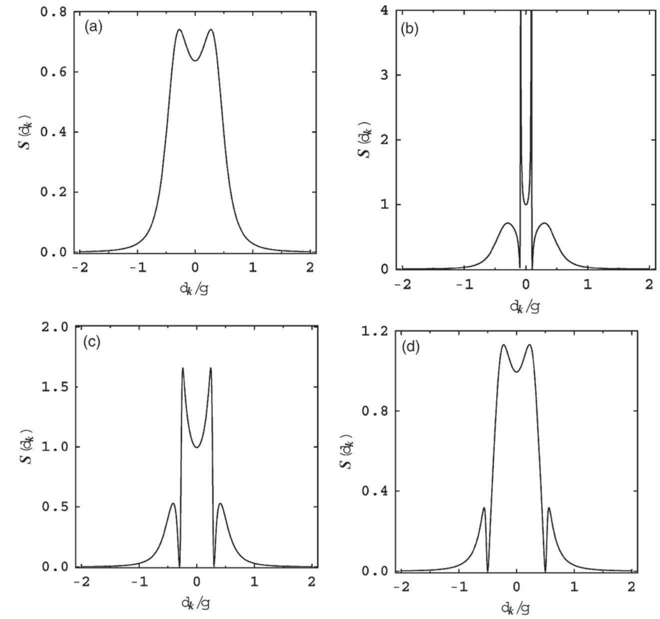

FIG. 3. The spontaneous emission spectra $S(\delta_k)$ (in units of γ^{-1}) for $\Omega_p=0.4\gamma$, $\Omega_c=0.2\gamma$, $a_g(0)=1$, $a_1(0)=a_2(0)=a_3(0)=0$, $\Gamma=\gamma$, and $\Delta_p=\Delta_c=\Delta_{\mathrm{rf}}=0$. (a) $\Omega_{\mathrm{rf}}=0$; (b) $\Omega_{\mathrm{rf}}=0.1\gamma$; (c) $\Omega_{\mathrm{rf}}=0.3\gamma$; and (d) $\Omega_{\mathrm{rf}}=0.5\gamma$.

quency detuning Δ_{rf} of the rf-driving field and vice versa.

Figure 3 shows the effect of rf field intensity on the spontaneous emission spectra $S(\delta_k)$ when the probe, coupling, and rf-driving fields are, respectively, tuned to the resonant interaction with the atomic transitions $|g\rangle\leftrightarrow|3\rangle$, $|2\rangle\leftrightarrow|3\rangle$, and $|1\rangle\leftrightarrow|2\rangle$. As can be seen, the change of the rf field intensity affects appreciably both the width of spectral lines and the position of the spontaneous emission quenching. For this case, the generated two fluorescence-quenching points are always located at $\delta_k=\pm|\Omega_{\mathrm{rf}}|$. We also find that only when the rf-driving field intensity is adjusted to the appropriate value, is the quantum interference between $|+\rangle\rightarrow|e\rangle$, $|0\rangle\rightarrow|e\rangle$, and $|-\rangle\rightarrow|e\rangle$ in the dressed states [see Eqs. (10a)–(10c) below] so strong that we can observe two extremely narrow and greatly enhanced spectral lines as shown in Fig. 3(b). With further increase of the intensity of the rf-driving field, we can see that two ultranarrow spectral lines become much wider and lower because this quantum interference similar to SGC [as discussed below, see Eqs. (12a)–(12e)] becomes much weaker. Specifically, for the case that no rf-driving field exists ($\Omega_{\mathrm{rf}}=0$), the spontaneous emission spectra exhibit symmetrical double-peak structure with equal height and normal linewidth restricted by spontaneous decay rate Γ [see Fig. 3(a)]. In contrast, when the rf field is applied, for the case that $\Omega_{\mathrm{rf}}=0.1\gamma$, the effect of the rf field is seen to cause a further splitting in each of the dynamic Stark components and gives rise to a four-peak spectral feature with two ultranarrow central lines and two normal width sideband lines. When the rf field intensity continues to increase [e.g., $\Omega_{\mathrm{rf}}=0.3\gamma$ and $\Omega_{\mathrm{rf}}=0.5\gamma$ in Figs. 3(c) and 3(d)], two central ultranarrow spectral lines with equal height become wider and lower; in the meantime two sideband spectral lines with equal height become narrower and lower. As expected, two ultranarrow sideband spectral lines with sufficiently low height can occur provided that the rf-field intensity is strong enough.

In order to further show the influence of the initial probability amplitudes on the spontaneous emission spectra $S(\delta_k)$, we give the corresponding curves in Fig. 4. The specific results are as follows. For the case that $a_g(0)=1$ and $a_1(0)=a_2(0)=a_3(0)=0$, two fluorescence-quenching points exist in the spontaneous emission spectra, located at $\delta_k=\pm0.2\gamma$. Alternatively, an ultranarrow spectral line can be observed at a fluorescence-quenching point $\delta_k=0.2\gamma$ [see Fig. 4(a)]. For the case that $a_g(0)=a_1(0)=1/\sqrt{2}$ and $a_2(0)=a_3(0)=0$, we can observe an extremely narrow and greatly enhanced spectral line [see Fig. 4(b)]. For the case that $a_g(0)=a_2(0)=1/\sqrt{2}$ and $a_1(0)=a_3(0)=0$, an ultranarrow central line and two normal width sideband lines occur in the spontaneous emission spectra [see Fig. 4(c)]. When the initial probability amplitudes subject to $a_1(0)=a_2(0)=1/\sqrt{2}$ and $a_g(0)=a_3(0)=0$, no ultranarrow line arises and the spontaneous emission spectra are singly peaked with normal width [see Fig. 4(d)]. With $a_3(0)=1$ and $a_g(0)=a_1(0)=a_2(0)=0$, we show the circumstance where three fluorescence-quenching points exist in the spontaneous emission spectra. It is clear that an ultranarrow line can be observed, where the two fluorescence-quenching points lie close together. Other three normal width sideband lines are located at both sides of the ultranarrow line [see Fig. 4(e)].

IV. ANALYSIS IN THE DRESSED-STATE PICTURE

In order to explicitly illustrate that the atomic system under consideration can be used as a substitution of a five-level

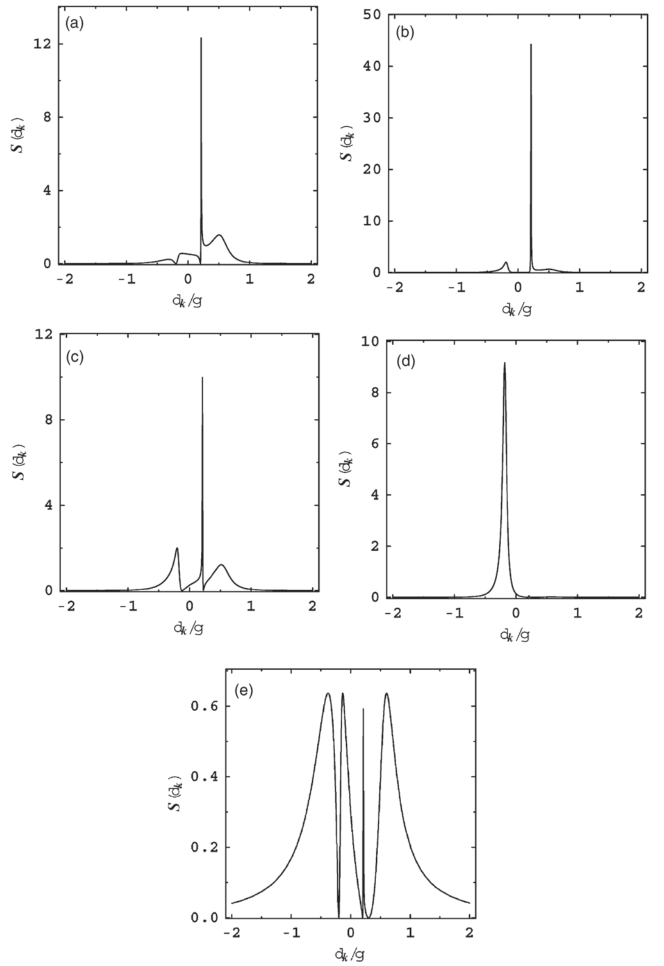

FIG. 4. The spontaneous emission spectra $S(\delta_k)$ (in units of γ^{-1}) for $\Omega_p=0.4\gamma$, $\Omega_c=0.2\gamma$, $\Omega_{\rm rf}=0.2\gamma$, $\Gamma=\gamma$, $\Delta_c=\Delta_{\rm rf}=0$, and $\Delta_p=0.3\gamma$. (a) $a_g(0)=1$ and $a_1(0)=a_2(0)=a_3(0)=0$; (b) $a_g(0)=a_1(0)=1/\sqrt{2}$ and $a_2(0)=a_3(0)=0$; (c) $a_g(0)=a_2(0)=1/\sqrt{2}$ and $a_1(0)=a_3(0)=0$; (d) $a_1(0)=a_2(0)=1/\sqrt{2}$ and $a_g(0)=a_3(0)=0$; and (e) $a_3(0)=1$ and $a_g(0)=a_1(0)=a_2(0)=0$.

atomic system with SGC effect in Ref. [34], we will turn our attention to the dressed-state picture, generated by the rf-driving field $\Omega_{\rm rf}$ and the coupling field Ω_c [47], namely, the $|1\rangle \leftrightarrow |2\rangle \leftrightarrow |3\rangle$ transitions together with the rf-driving and coupling fields are treated as a coupled "atom+field" system and the energy levels of the dressed states form a ladder of triplets as shown in Fig. 1(b). It is obvious that bare-state level $|3\rangle$ should be split into three dressed-state sublevels $|\pm\rangle$ and $|0\rangle$. The energy eigenvalues of the three dressed states for the two-photon resonant case that $\Delta_c+\Delta_{\rm rf}=0$ are given by

$$\lambda_{\pm}=\frac{\Delta_{\rm rf}\pm\sqrt{\Delta_{\rm rf}^2+4(\Omega_c^2+\Omega_{\rm rf}^2)}}{2} \quad \text{and} \quad \lambda_0=0. \tag{9}$$

The corresponding energy eigenstates are written as

$$|+\rangle=(\sin\theta)\sin\phi|3\rangle+\cos\phi|2\rangle+(\cos\theta)\sin\phi|1\rangle, \tag{10a}$$

$$|0\rangle=\cos\theta|3\rangle-\sin\theta|1\rangle, \tag{10b}$$

$$|-\rangle=(\sin\theta)\cos\phi|3\rangle-\sin\phi|2\rangle+(\cos\theta)\cos\phi|1\rangle, \tag{10c}$$

with

$$\sin\phi=\frac{\sqrt{\Omega_c^2+\Omega_{\rm rf}^2}}{\sqrt{\lambda_+^2+\Omega_c^2+\Omega_{\rm rf}^2}}=-\frac{\lambda_-}{\sqrt{\lambda_-^2+\Omega_c^2+\Omega_{\rm rf}^2}},$$

$$\cos\phi=\frac{\lambda_+}{\sqrt{\lambda_+^2+\Omega_c^2+\Omega_{\rm rf}^2}}=\frac{\sqrt{\Omega_c^2+\Omega_{\rm rf}^2}}{\sqrt{\lambda_-^2+\Omega_c^2+\Omega_{\rm rf}^2}},$$

$$\sin\theta=\frac{\Omega_c}{\sqrt{\Omega_c^2+\Omega_{\rm rf}^2}}, \quad \text{and} \quad \cos\theta=\frac{\Omega_{\rm rf}}{\sqrt{\Omega_c^2+\Omega_{\rm rf}^2}}.$$

According to the above dressed states (10a)–(10c), the probability amplitudes of the bare states are associated with the probability amplitudes of the dressed states by the following relations

$$a_1(t)=(\cos\theta)\sin\phi a_+(t)-(\sin\theta)a_0(t)+(\cos\theta)\cos\phi a_-(t), \tag{11a}$$

$$a_2(t)=\cos\phi a_+(t)-\sin\phi a_-(t), \tag{11b}$$

$$a_3(t)=(\sin\theta)\sin\phi a_+(t)+(\cos\theta)a_0(t)+(\sin\theta)\cos\phi a_-(t). \tag{11c}$$

Making full use of the above expressions (11a)–(11c), after some algebraic calculations Eqs. (4a)–(4e) can then be rewritten as

$$\frac{\partial a_g(t)}{\partial t}=-i\Omega_{p+}a_+(t)-i\Omega_{p0}a_0(t)-i\Omega_{p-}a_-(t), \tag{12a}$$

$$\frac{\partial a_+(t)}{\partial t}=-\left[i(\Delta_p+\lambda_+)+\frac{\Gamma_+}{2}\right]a_+(t)-i\Omega_{p+}a_g(t)-\frac{\sqrt{\Gamma_+\Gamma_-}}{2}a_-(t)-\frac{\sqrt{\Gamma_+\Gamma_0}}{2}a_0(t), \tag{12b}$$

$$\frac{\partial a_0(t)}{\partial t}=-\left(i\Delta_p+\frac{\Gamma_0}{2}\right)a_0(t)-i\Omega_{p0}a_g(t)-\frac{\sqrt{\Gamma_0\Gamma_+}}{2}a_+(t)-\frac{\sqrt{\Gamma_0\Gamma_-}}{2}a_-(t), \tag{12c}$$

$$\frac{\partial a_-(t)}{\partial t}=-\left[i(\Delta_p+\lambda_-)+\frac{\Gamma_-}{2}\right]a_-(t)-i\Omega_{p-}a_g(t)-\frac{\sqrt{\Gamma_-\Gamma_+}}{2}a_+(t)-\frac{\sqrt{\Gamma_-\Gamma_0}}{2}a_0(t), \tag{12d}$$

$$\frac{\partial a_k(t)}{\partial t}=-i(\Delta_p-\delta_k)a_k(t)-ig_{k+}^{*}a_+(t)-ig_{k0}^{*}a_0(t)-ig_{k-}^{*}a_-(t), \tag{12e}$$

where $\Omega_{p+}=\Omega_p(\sin\theta)\sin\phi$, $\Omega_{p0}=\Omega_p\cos\theta$, $\Omega_{p-}=\Omega_p(\sin\theta)\cos\phi$, $\Gamma_+=\Gamma(\sin^2\theta)\sin^2\phi$, $\Gamma_0=\Gamma\cos^2\theta$,

$\Gamma_- = \Gamma(\sin^2\theta)\cos^2\phi$, $g_{k+} = g_k(\sin\theta)\sin\phi$, $g_{k0} = g_k\cos\theta$, and $g_{k-} = g_k(\sin\theta)\cos\phi$. λ_+ and λ_- are directly determined by the expression (9).

From the above equations (12b)–(12d), it is straightforward to show that there exists quantum interference between three different spontaneous emission pathways $|+\rangle \to |e\rangle$, $|0\rangle \to |e\rangle$, and $|-\rangle \to |e\rangle$, which are in good agreement with the results given in Ref. [34]. Therefore, it is obvious that the atomic system studied here is equivalent in form to just such a five-level atomic system with SGC as investigated in Ref. [34]. The only difference is that the three close-lying levels are dressed states, but not real atomic states as in Ref. [34]. As we well know, it is very difficult to seek a real atomic system matching the conditions of SGC and then carry out corresponding experiments related to SGC. Adopting our proposed scheme, however, it is feasible to observe the expected singular phenomena based on SGC in experiment, because no specific conditions are required to be fulfilled.

Before ending this section, let us briefly discuss the possible experimental realization of our proposed scheme by means of alkali-metal atoms, appropriate diode lasers, and microwave source. Specifically, we consider, for instance, the cold atoms $^{87}\mathrm{Rb}-D_2$ line (nuclear spin $I=3/2$) as a possible candidate. The designated states can be chosen as follows: $|g\rangle = |5S_{1/2}, F=1, m_F=1\rangle$, $|1\rangle = |5S_{1/2}, F=1, m_F=0\rangle$, $|2\rangle = |5S_{1/2}, F=2, m_F=0\rangle$, $|e\rangle = |5S_{1/2}, F=2, m_F=2\rangle$, and $|3\rangle = |5P_{3/2}, F=2, m_F=1\rangle$, respectively. In this case, the coherent probe and coupling fields can be obtained from external cavity diode lasers. A microwave field drives the magnetic dipole transition between $|1\rangle = |5S_{1/2}, F=1, m_F=0\rangle$ and $|2\rangle = |5S_{1/2}, F=2, m_F=0\rangle$ with the hyperfine splitting frequency $\omega_{12} \simeq 6.84$ GHz, while the transition from the excited level $|3\rangle = |5P_{3/2}, F=2, m_F=1\rangle$ to the metastable level $|e\rangle = |5S_{1/2}, F=2, m_F=2\rangle$ can be coupled by the vacuum modes in the free space. The probe and coupling fields are linearly and right circularly polarized, respectively. Moreover, in order to eliminate the Doppler broadening effect, atoms should be trapped and cooled by the magneto-optical trap (MOT) technique.

V. CONCLUSIONS

To summarize, we have theoretically investigated the spontaneous emission spectra of a coherently driven five-level atomic system without close-lying levels by means of an rf field driving a hyperfine transition within the ground state. The results clearly show that, by properly adjusting the frequency detuning and intensity of the rf-driving field, we can observe a few interesting phenomena in the spontaneous emission spectra, such as spectral-line narrowing, spectral-line enhancement, spectral-line suppression, and spontaneous emission quenching. The observed singular spontaneous emission spectra can be regarded as results of multiple SGC in the dressed-state picture. The influence of the initial probability amplitudes on the spontaneous emission spectra is also analyzed.

According to our analysis, these interesting phenomena should be observable in realistic experiments by using alkali-metal atoms (e.g., cold Rb or Na atoms) in a MOT where the atomic temperature can be decreased to several tens of μK so that the Doppler broadening effect can be effectively eliminated, using the appropriate diode lasers and microwave source. If the atoms are in a cell, however, it is certain that velocity distributions or decay terms due to the interaction with a buffer gas have to be included, and some phenomena described in this paper will be significantly modified, although the underlying physics of quantum interference and atomic coherence is still valid. We are currently carrying out exact calculations on the spontaneous emissions spectra from atoms in a cell both with and without a buffer gas.

Finally, it is pointed out that we do not consider the effect of atomic motion and hence, there is the Doppler-free broadening effect in our treatment. Consequently, the results here are suitable only for the cold atoms.

ACKNOWLEDGMENTS

The research is supported in part by the National Natural Science Foundation of China (Grant Nos. 10575040, 90503010, and 60478029) and by the National Basic Research Program of China under Contract No. 2005CB724508. The authors would like to thank Professor Ying Wu for helpful discussion and his encouragement.

[1] S. Y. Zhu, H. Chen, and H. Huang, Phys. Rev. Lett. **79**, 205 (1997).
[2] S. John and T. Quang, Phys. Rev. Lett. **78**, 1888 (1997).
[3] P. Zhou and S. Swain, Phys. Rev. A **55**, 772 (1997).
[4] C. H. Keital, P. L. Knight, L. M. Narducci, and M. O. Scully, Opt. Commun. **118**, 143 (1995).
[5] F. Ghafoor, S. Y. Zhu, and M. S. Zubairy, Phys. Rev. A **62**, 013811 (2000).
[6] E. Paspalakis, C. H. Keitel, and P. L. Knight, Phys. Rev. A **58**, 4868 (1998).
[7] E. Paspalakis and P. L. Knight, Phys. Rev. Lett. **81**, 293 (1998); E. Paspalakis, N. J. Kylstra, and P. L. Knight, *ibid.* **82**, 2079 (1999); E. Paspalakis, N. J. Kylstra, and P. L. Knight, Phys. Rev. A **61**, 045802 (2000).
[8] M. A. Antón, O. G. Calderón, and F. Carreño, Phys. Rev. A **72**, 023809 (2005); X. M. Hu and J. S. Peng, J. Phys. B **33**, 921 (2000); X. M. Hu, W. X. Shi, Q. Xu, H. J. Guo, J. Y. Li, and X. X. Li, Phys. Lett. A **352**, 543 (2006).
[9] H. Lee, P. Polynkin, M. O. Scully, and S. Y. Zhu, Phys. Rev. A **55**, 4454 (1997).
[10] S. Y. Zhu and M. O. Scully, Phys. Rev. Lett. **76**, 388 (1996).
[11] P. Zhou and S. Swain, Phys. Rev. Lett. **78**, 832 (1997).
[12] Y. Wu and X. Yang, Phys. Rev. A **70**, 053818 (2004).
[13] T. Hong, C. Cramer, W. Nagourney, and E. N. Fortson, Phys. Rev. Lett. **94**, 050801 (2005).
[14] F. Ghafoor, S. Qamar, and M. S. Zubairy, Phys. Rev. A **65**,

043819 (2002).
[15] M. A. G. Martinez, P. R. Herczfeld, C. Samuels, L. M. Narducci, and C. H. Keitel, Phys. Rev. A **55**, 4483 (1997).
[16] G. S. Agarwal, Phys. Rev. Lett. **67**, 980 (1991).
[17] A. S. Zibrov, M. D. Lukin, D. E. Nikonov, L. Hollberg, M. O. Scully, V. L. Velichansky, and H. G. Robinson, Phys. Rev. Lett. **75**, 1499 (1995).
[18] S. E. Harris, Phys. Rev. Lett. **62**, 1033 (1989).
[19] J. Y. Gao, C. Guo, X. Z. Guo, G. X. Jin, Q. W. Wang, J. Zhao, H. Z. Zhang, Y. Jiang, D. Z. Wang, and D. M. Jiang, Opt. Commun. **93**, 323 (1992).
[20] M. O. Scully and M. Fleischhauer, Phys. Rev. Lett. **69**, 1360 (1992).
[21] M. Fleischhauer, A. B. Matsko, and M. O. Scully, Phys. Rev. A **62**, 013808 (2000).
[22] T. Hong, C. Cramer, W. Nagourney, and E. N. Fortson, Phys. Rev. Lett. **94**, 050801 (2005).
[23] M. O. Scully, Phys. Rev. Lett. **67**, 1855 (1991).
[24] M. Fleischhauer, C. H. Keitel, M. O. Scully, C. Su, B. T. Ulrich, and S. Y. Zhu, Phys. Rev. A **46**, 1468 (1992).
[25] C. H. Bennett and D. P. Divincenzo, Nature (London) **404**, 247 (2000).
[26] D. Petrosyan and Y. P. Malakyan, Phys. Rev. A **70**, 023822 (2004).
[27] M. Paternostro, M. S. Kim, and P. L. Knight, Phys. Rev. A **71**, 022311 (2005).
[28] E. Arimondo, in *Progress in Optics*, edited by E. Wolf (Elsevier, Amsterdam, 1996), p. 257.
[29] G. S. Agarwal, *Quantum Optics* (Springer-Verlag, Berlin, 1974), p. 68.
[30] G. X. Li, F. L. Li, and S. Y. Zhu, Phys. Rev. A **64**, 013819 (2001).
[31] For early work on this subject, see also G. S. Agarwal, Phys. Rev. Lett. **84**, 5500 (2000).
[32] J. H. Wu, A. J. Li, Y. Ding, Y. C. Zhao, and J. Y. Gao, Phys. Rev. A **72**, 023802 (2005).
[33] A. J. Li, J. Y. Gao, J. H. Wu, and L. Wang, J. Phys. B **38**, 3815 (2005).
[34] A. Fountoulakis, A. F. Terzis, and E. Paspalakis, Phys. Rev. A **73**, 033811 (2006).
[35] M. D. Lukin, S. F. Yelin, M. Fleischhauer, and M. O. Scully, Phys. Rev. A **60**, 3225 (1999).
[36] Y. C. Chen, Y. A. Liao, H. Y. Chiu, J. J. Su, and I. A. Yu, Phys. Rev. A **64**, 053806 (2001).
[37] Y. Niu, S. Gong, R. Li, and S. Jin, Phys. Rev. A **70**, 023805 (2004).
[38] Y. Niu, R. Li, and S. Gong, Phys. Rev. A **71**, 043819 (2005).
[39] C. Y. Ye, A. S. Zibrov, Y. V. Rostovtsev, and M. O. Scully, Phys. Rev. A **65**, 043805 (2002).
[40] S. F. Yelin, V. A. Sautenkov, M. M. Kash, G. R. Welch, and M. D. Lukin, Phys. Rev. A **68**, 063801 (2003).
[41] A. M. Akulshin, S. Barreiro, and A. Lezama, Phys. Rev. A **57**, 2996 (1998); S. Brattkea, U. Kallmann, and W. D. Hartmannb, Eur. Phys. J. D **3**, 159 (1998); S. Knappe *et al.*, J. Opt. Soc. Am. B **18**, 1545 (2001); C. Y. Ye and A. S. Zibrov, Phys. Rev. A **65**, 023806 (2002); A. Javan, O. Kocharovskaya, H. Lee, and M. O. Scully, Phys. Rev. A **66**, 013805 (2002).
[42] C. Goren, A. D. Wilson-Gordon, M. Rosenbluh, and H. Friedmann, Phys. Rev. A **69**, 063802 (2004).
[43] E. Paspalakis, N. J. Kylstra, and P. L. Knight, Phys. Rev. A **65**, 053808 (2002); E. Paspalakis and P. L. Knight, J. Opt. B: Quantum Semiclassical Opt. **4**, 372 (2002).
[44] Y. Wu, J. Saldana, and Y. Zhu, Phys. Rev. A **67**, 013811 (2003); Y. Wu, L. Wen, and Y. Zhu, Opt. Lett. **28**, 631 (2003).
[45] Y. Wu and X. Yang, Phys. Rev. A **71**, 053806 (2005).
[46] S. M. Barnett and P. M. Radmore, *Methods in Theoretical Quantum Optics* (Oxford University Press, Oxford, 1997), p. 140.
[47] Without loss of generality, we have assumed that the rf-driving field Ω_{rf} and the coupling field Ω_c are real in this section.